

Thermal relaxation model of surface director gliding in lyotropic liquid crystals

P. Galatola and G. Barbero

Dipartimento di Fisica del Politecnico di Torino and Istituto Nazionale di Fisica della Materia, Corso Duca degli Abruzzi 24, I-10129 Torino, Italy

A. K. Zvezdin

Institute of General Physics of the Russian Academy of Sciences, Vavilov Street 38, 117942 Moscow, Russia

(Received 4 November 1996)

The gliding of the nematic director at an isotropic surface in a lyotropic liquid crystal, induced by a magnetic field, is theoretically analyzed by means of a thermal relaxation model. We formulate a master-equation describing the process and we derive a Fokker-Planck approximation from which simple analytical results are obtained. The relaxation time is found to be inversely proportional to the square of the magnetic field, in agreement with recent experimental measurements. The observed temperature dependence of the relaxation time is explained in the framework of a simple mean-field model in which the surface energy is supposed to be proportional to the bulk nematic order parameter. [S1063-651X(97)10303-8]

PACS number(s): 61.30.Gd, 02.50.Ey

I. INTRODUCTION

Nematic liquid crystals are uniaxial mesogens formed by rodlike elongated constituents [1]. These elementary constituents are molecules in the case of *thermotropics*, where the mesogenic behavior is controlled by the temperature, and *micelles* in the case of *lyotropics* [2], in which the mesogenic behavior is determined by the concentration. Nematic liquid-crystal samples can be oriented by applying external electric or magnetic fields [1]. The resulting equilibrium director configuration depends on the boundary conditions at the surfaces of the sample.

In the past, the anchoring properties of thermotropic nematic liquid crystals have been thoroughly analyzed both theoretically and experimentally [3]. In particular, it has been shown that in the case of polyvinyl-alcohol-rubbed surfaces—giving a homogeneous weak planar anchoring—the experimental data are compatible with a zero value of the static friction torque [4]. This result, obtained for a particular surface treatment, is actually more general. In fact, in thermotropic liquid crystals all the known surface orientational effects are reversible: removing the distorting field, the sample recovers the original orientational state [1]. On the contrary, in lyotropic liquid crystals, it has been recently observed that a slow gliding of a planar degenerate surface orientation can be induced by an external orienting magnetic field of the order of only a few kilogauss [5–7]. This irreversible process has been interpreted by means of a phenomenological model, by supposing that at the surface a bilayer of amphiphilic molecules is present, with defects or channels as in a micellar structure [5]. This model explains the observed dependence of the relaxation time on the amplitude of the applied magnetic field, but, in order to fit the order of magnitude of these relaxation times, one must introduce an effective surface viscosity connected to the bulk one by the macroscopic dimension of the objects that are supposed to rigidly participate to the surface orienting phenomenon.

In this paper we propose a microscopic approach to the surface gliding effect in terms of a thermally activated process. According to this model, the micelles are rotationally

pinned to the surface by a potential displaying successive local minima in correspondence with metastable orientational states. For simplicity, we shall assume that the potential is periodic, with equispaced minima separated by the same potential barrier U_0 [see Fig. 1(a)]. In the absence of external orienting fields, the surface micelles rotate against the potential barriers with an attempt frequency τ_0^{-1} and they succeed in overcoming the barrier with a rate $\tau^{-1} = \tau_0^{-1} \exp[-U_0/(K_B T)] \ll \tau_0^{-1}$. During the jump from one metastable state to the adjacent one, a bunch of phonons is radiated, leading to an irreversible process. These jumps give rise to a uniform *diffusion*, which is contrasted, as we shall see in the following, by the elasticity of the nematic liquid crystal. An equilibrium surface distribution of angles at the surface results, which is rotationally invariant: the mean surface twist angle depends only on the initial conditions. In the presence of an external magnetic field the rotational symmetry of the surface potential is broken [see Fig. 1(b)]: the transition probability for rotation in the direction of the field is higher than in the opposite direction. Hence a *drift* of the initial probability distribution in the direction of the field occurs, giving rise to the gliding process. The relaxation times are expected to be much longer than the characteristic thermal equilibration time τ , as they result from the small imbalance of the potential barriers introduced by the presence of the field. This model of the surface gliding is reminiscent of the solid friction model involving the pinning between the asperities of two solid surfaces in contact [8].

In Sec. II we derive a mean-field model for the surface molecular energy. A master equation describing the gliding process is formulated in Sec. III along with a Fokker-Planck approximation in the continuum limit. Numerical and approximate analytical results are discussed in Sec. IV: the dependence of the relaxation time on the applied magnetic field is obtained. The temperature dependence of the relaxation time is discussed in Sec. V in the framework of a mean-field approach. A comparison with the experimental data is presented, showing good agreement. In Sec. VI we summarize our results and outline some possible generalizations.

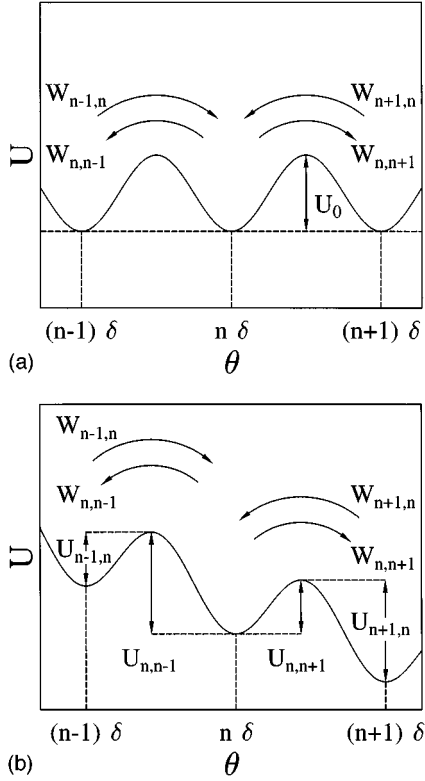


FIG. 1. Schematic representation of the surface potential in the (a) absence and (b) presence of an orienting magnetic field. An extra elastic contribution is actually present, which contrasts with the diffusion in the absence of field.

II. SURFACE MOLECULAR ENERGY MODEL

Let us consider a semi-infinite nematic lyotropic sample extending in the region $z > 0$ of a Cartesian coordinate frame, with the $z=0$ plane coincident with an isotropic solid substrate. A magnetic field \mathbf{H} is applied parallel to the (x,y) substrate plane at an angle θ_H with respect to the x axis. We suppose that the nematic lyotropic sample can be modeled as an assembly of layers, parallel to the solid substrate, having a thickness l comparable with the molecular short diameter. Each layer is labeled with an index $i=0,1,2,\dots$, where the zeroth layer is the one in contact with the substrate.

We make an Ising-like mean-field model [9] for the interaction between the layers. Therefore, for a given bulk layer $i > 0$, we write the total energy per unit surface g_i as

$$g_i = -J[(\langle \hat{\mathbf{n}}_i \rangle \cdot \langle \hat{\mathbf{n}}_{i+1} \rangle)^2 + (\langle \hat{\mathbf{n}}_i \rangle \cdot \langle \hat{\mathbf{n}}_{i-1} \rangle)^2] - J' \sum_{k=1}^N (\hat{\mathbf{n}}_i^{(k)} \cdot \langle \hat{\mathbf{n}}_i \rangle)^2 - \frac{1}{2} \frac{\chi_{am}}{NA} \sum_{k=1}^N (\hat{\mathbf{n}}_i^{(k)} \cdot \mathbf{H})^2. \quad (2.1)$$

Here $\hat{\mathbf{n}}_i^{(k)}$ is the nematic director for the k th micelle in the i th layer; $\langle \hat{\mathbf{n}}_i \rangle$ is its average in the layer; J is the coupling constant between adjacent layers; J' is the self-coupling in each layer, favoring a homogeneous orientation; χ_{am} is the micellar diamagnetic anisotropy, which we suppose positive; and finally, N is the number of micelles in each layer and

At the area occupied by each micelle. Similarly, we can write the total energy per unit surface g_0 of the layer in contact with the solid substrate as

$$g_0 = -J(\langle \hat{\mathbf{n}}_0 \rangle \cdot \langle \hat{\mathbf{n}}_1 \rangle)^2 - J' \sum_{k=1}^N (\hat{\mathbf{n}}_0^{(k)} \cdot \langle \hat{\mathbf{n}}_0 \rangle)^2 - \frac{1}{2} \frac{\chi_{am}}{NA} \sum_{k=1}^N (\hat{\mathbf{n}}_0^{(k)} \cdot \mathbf{H})^2 + U_0, \quad (2.2)$$

where U_0 accounts for the interaction between the surface layer and the substrate.

In the following we assume that all the micelles lie everywhere parallel to the (x,y) plane, such that

$$\hat{\mathbf{n}}_i^{(k)} = \cos \theta_i^{(k)} \hat{\mathbf{x}} + \sin \theta_i^{(k)} \hat{\mathbf{y}}, \quad (2.3a)$$

$$\langle \hat{\mathbf{n}}_i \rangle = \cos \bar{\theta}_i \hat{\mathbf{x}} + \sin \bar{\theta}_i \hat{\mathbf{y}}, \quad (2.3b)$$

where $\hat{\mathbf{x}}$ and $\hat{\mathbf{y}}$ are the x - and y -axis unit versors, respectively. Therefore,

$$\sum_{k=1}^N (\hat{\mathbf{n}}_i^{(k)} \cdot \langle \hat{\mathbf{n}}_i \rangle)^2 = N \langle \cos^2(\theta_i - \bar{\theta}_i) \rangle, \quad (2.4a)$$

$$\sum_{k=1}^N (\hat{\mathbf{n}}_i^{(k)} \cdot \hat{\mathbf{H}})^2 = NH^2 \langle \cos^2(\theta_i - \theta_H) \rangle. \quad (2.4b)$$

We now make the expansion

$$\bar{\theta}_{i\pm 1} \cong \bar{\theta}_i \pm \frac{d\bar{\theta}_i}{dz} l, \quad (2.5)$$

from which it follows that

$$(\langle \hat{\mathbf{n}}_i \rangle \cdot \langle \hat{\mathbf{n}}_{i\pm 1} \rangle)^2 = \cos^2(\bar{\theta}_i - \bar{\theta}_{i\pm 1}) \cong 1 - \left(\frac{d\bar{\theta}_i}{dz} \right)^2 l^2. \quad (2.6)$$

Consequently, apart from inessential constants,

$$g_i = 2Jl^2 \left(\frac{d\bar{\theta}_i}{dz} \right)^2 - J' N \langle \cos^2(\theta_i - \bar{\theta}_i) \rangle - \frac{1}{2} \frac{\chi_{am}}{A} H^2 \langle \cos^2(\theta_i - \theta_H) \rangle \quad (2.7)$$

and

$$g_0 = Jl^2 \left(\frac{d\bar{\theta}_0}{dz} \right)^2 - J' N \langle \cos^2(\theta_0 - \bar{\theta}_0) \rangle - \frac{1}{2} \frac{\chi_{am}}{A} H^2 \langle \cos^2(\theta_0 - \theta_H) \rangle + U_0. \quad (2.8)$$

To connect the microscopic parameters entering in Eqs. (2.7) and (2.8) with the usual macroscopic constants appearing in the framework of the continuum elastic theory [10], we write

$$\theta_i^{(k)} = \bar{\theta}_i + \Delta \theta_i^{(k)}, \quad (2.9)$$

where by definition $\langle \Delta \theta_i \rangle = 0$, such that

$$\langle \cos^2(\theta_i - \bar{\theta}_i) \rangle \cong 1 - \langle \Delta \theta_i^2 \rangle \quad (2.10)$$

and

$$\begin{aligned} \langle \cos^2(\theta_i - \theta_H) \rangle &= \langle \cos^2(\bar{\theta}_i - \theta_H + \Delta \theta_i) \rangle \\ &\cong \langle \cos^2(\bar{\theta}_i - \theta_H) - \sin[2(\bar{\theta}_i - \theta_H)] \Delta \theta_i \rangle \\ &= \cos^2(\bar{\theta}_i - \theta_H). \end{aligned} \quad (2.11)$$

Consequently, the total energy per unit surface of the i th bulk layer (2.7) becomes, apart from inessential constant terms,

$$g_i = 2Jl^2 \left(\frac{d\bar{\theta}_i}{dz} \right)^2 + J'N \langle \Delta \theta_i^2 \rangle - \frac{1}{2} \frac{\chi_{am}}{A} H^2 \cos^2(\bar{\theta}_i - \theta_H). \quad (2.12)$$

According to the continuum elastic theory, in the one-constant approximation the bulk energy density is [1]

$$f = \frac{1}{2} K (\nabla \theta)^2 - \frac{1}{2} \chi_a H^2 \cos^2(\theta - \theta_H), \quad (2.13)$$

where K is the usual Frank elastic constant and χ_a the diamagnetic anisotropy. In our geometry, where θ mainly depends on the distance z from the surface, we can make the approximation

$$(\nabla \theta)^2 = \left(\frac{\partial \theta}{\partial x} \right)^2 + \left(\frac{\partial \theta}{\partial y} \right)^2 + \left(\frac{\partial \theta}{\partial z} \right)^2 \cong \frac{\langle \Delta \theta^2 \rangle}{A} + \left(\frac{\partial \theta}{\partial z} \right)^2. \quad (2.14)$$

By comparing Eq. (2.12) with lf given by Eqs. (2.13) and (2.14), we arrive at

$$J = \frac{K}{4l}, \quad J' = \frac{Kl}{2NA}, \quad \chi_{am} = \chi_a Al. \quad (2.15)$$

By neglecting in Eq. (2.13) the small variations of the twist angle θ in the (x, y) plane, standard calculations give for the actual stable profile [1]

$$\left(\frac{d\theta}{dz} \right)^2 = \frac{\chi_a H^2}{K} \sin^2(\theta - \theta_H). \quad (2.16)$$

Then, from Eq. (2.8) we have

$$g_0 A = \langle \mathcal{U} \rangle, \quad (2.17)$$

where \mathcal{U} can be identified as the total energy of a surface micelle

$$\begin{aligned} \mathcal{U} &= \frac{1}{4} \chi_{am} H^2 \sin^2(\bar{\theta}_0 - \theta_H) + \frac{1}{2} \chi_{am} H^2 \sin^2(\theta_0 - \theta_H) \\ &\quad - \frac{1}{2} Kl \cos^2(\theta_0 - \bar{\theta}_0) + \mathcal{U}_0, \end{aligned} \quad (2.18)$$

with $\mathcal{U}_0 = U_0 A$.

III. MASTER EQUATION AND FOKKER-PLANCK APPROXIMATION

Let us suppose that the possible angular positions of the surface micelles are quantized according to

$$\theta_n = n \delta \quad (n = 0, \pm 1, \pm 2, \dots). \quad (3.1)$$

We call P_n the probability to find a micelle with the orientation θ_n . Evidently, the time evolutions of the probabilities obey the *master equation*

$$\frac{dP_n}{dt} = W_{n-1,n} P_{n-1} + W_{n+1,n} P_{n+1} - (W_{n,n-1} + W_{n,n+1}) P_n, \quad (3.2)$$

where $W_{n,m}$ is the transition probability between two adjacent angles θ_n and θ_m , with $n - m = \pm 1$ (see Fig. 1). According to statistical mechanics [9]

$$W_{m,m\pm 1} = \frac{1}{\tau_0} \exp \left[\frac{\mathcal{U}(m\delta) - \mathcal{U}[(m \pm 1/2)\delta]}{K_B T} \right], \quad (3.3)$$

where K_B is the Boltzmann constant, T the absolute temperature, and τ_0^{-1} the trial frequency. In Eq. (3.4) $\mathcal{U}[(m \pm 1/2)\delta] - \mathcal{U}(m\delta)$ represents the height of the barrier that a micelle has to overcome to jump between adjacent angular positions. For $\delta \ll 1$, according to Eq. (2.18), we can write

$$\begin{aligned} W_{m,m\pm 1} &= \frac{1}{\tau_0} \exp \left(-u_0 \mp \frac{1}{2} \{ h^2 \sin[2(\theta_m - \theta_H)] \right. \\ &\quad \left. + \kappa \sin[2(\theta_m - \bar{\theta})] \} \delta \right), \end{aligned} \quad (3.4)$$

where

$$u_0 = \frac{\mathcal{U}_0[(m \pm 1/2)\delta] - \mathcal{U}_0(m\delta)}{K_B T} \quad (3.5)$$

is the height of the barrier, which we suppose constant, between two adjacent angular positions due to the surface anchoring energy; h and κ are the normalized magnetic field and elastic constant, respectively,

$$h^2 = \frac{\chi_{am} H^2}{2K_B T}, \quad \kappa = \frac{Kl}{2K_B T}. \quad (3.6)$$

In Eq. (3.4) we have omitted the subscript 0 on the angles for the sake of simplicity. Note that in Eq. (3.4), the term proportional to h^2 is connected with the drift of the surface micelles toward θ_H , whereas the term proportional to κ contrasts with the diffusion. The height of the barrier u_0 renormalizes the trial frequency, allowing us to define the characteristic diffusion time

$$\tau = \tau_0 \exp(u_0). \quad (3.7)$$

The average surface twist angle $\bar{\theta}$ in Eq. (3.4) defines the direction of the macroscopic surface director, which is the eigenvector associated with the positive eigenvalue of the traceless surface order parameter

$$\mathbf{q} = 2 \left\langle \hat{\mathbf{n}} \otimes \hat{\mathbf{n}} - \frac{1}{2} \mathbf{I} \right\rangle, \quad (3.8)$$

where \mathbf{I} is the identity tensor. In the diagonal frame

$$\mathbf{q} = \begin{pmatrix} s & 0 \\ 0 & -s \end{pmatrix}, \quad (3.9)$$

where $0 \leq s \leq 1$ is the two-dimensional surface order parameter

$$s = \sqrt{(2\langle \cos^2 \theta \rangle - 1)^2 + \langle \sin(2\theta) \rangle^2}. \quad (3.10)$$

According to the previous definition

$$\bar{\theta} = \tan^{-1} \left[\frac{\langle \sin(2\theta) \rangle}{2\langle \cos^2 \theta \rangle + s - 1} \right]. \quad (3.11)$$

In the limit of small jumps $\delta \rightarrow 0$, we can perform the expansions

$$P_{n \pm 1} = P(\theta) \pm \frac{\partial P}{\partial \theta} \delta + \frac{1}{2} \frac{\partial^2 P}{\partial \theta^2} \delta^2, \quad (3.12a)$$

$$W_{n \pm 1, n} = W(\theta, \theta' = \theta) \pm \frac{\partial W}{\partial \theta} \delta + \frac{1}{2} \frac{\partial^2 W}{\partial \theta^2} \delta^2, \quad (3.12b)$$

$$W_{n, n \pm 1} = W(\theta, \theta' = \theta) \pm \frac{\partial W}{\partial \theta'} \delta + \frac{1}{2} \frac{\partial^2 W}{\partial \theta'^2} \delta^2, \quad (3.12c)$$

with

$$W(\theta, \theta' = \theta) = \frac{1}{\tau}, \quad (3.13a)$$

$$\frac{\partial W}{\partial \theta} = \frac{1}{2\tau} \frac{du}{d\theta}, \quad (3.13b)$$

$$\frac{\partial W}{\partial \theta'} = -\frac{1}{2\tau} \frac{du}{d\theta}, \quad (3.13c)$$

$$\frac{\partial^2 W}{\partial \theta^2} = \frac{1}{4\tau} \left(\frac{du}{d\theta} \right)^2 + \frac{1}{2\tau} \frac{d^2 u}{d\theta^2}, \quad (3.13d)$$

$$\frac{\partial^2 W}{\partial \theta'^2} = \frac{1}{4\tau} \left(\frac{du}{d\theta} \right)^2 - \frac{1}{2\tau} \frac{d^2 u}{d\theta^2}, \quad (3.13e)$$

where, according to Eq. (2.18),

$$u(\theta) = \frac{\mathcal{U} - \mathcal{U}_0}{K_B T} = \frac{1}{2} h^2 \sin^2(\bar{\theta} - \theta_H) + h^2 \sin^2(\theta - \theta_H) + \kappa \sin^2(\theta - \bar{\theta}). \quad (3.14)$$

In this continuum- θ approximation, the master equation (3.2) therefore reduces to the *Fokker-Planck* equation for the probability density $\mathcal{P}(\theta, t)$,

$$\frac{\partial \mathcal{P}}{\partial t'} = \frac{\partial}{\partial \theta} \left(\frac{du}{d\theta} \mathcal{P} \right) + \frac{\partial^2 \mathcal{P}}{\partial \theta^2}, \quad (3.15)$$

with $t' = Dt$ the normalized time, where D is the rotational surface diffusion coefficient

$$D = \lim_{\delta \rightarrow 0} \frac{\delta^2}{\tau}. \quad (3.16)$$

IV. ANALYTICAL AND NUMERICAL RESULTS

From the Fokker-Planck approximation (3.15), the steady-state solution [11] readily follows

$$\mathcal{P}_s(\theta) = \frac{\exp[-u(\theta)]}{\int_0^\pi \exp[-u(\theta)] d\theta}. \quad (4.1)$$

As expected, it is a Boltzmann distribution. For a sufficiently well-peaked distribution, we can set

$$\bar{\theta} \cong \langle \theta \rangle = \int_0^\pi \theta \mathcal{P}(\theta) d\theta \quad (4.2)$$

such that, from Eq. (3.15),

$$\frac{d\bar{\theta}}{dt'} = - \left\langle \frac{du}{d\theta} \right\rangle. \quad (4.3)$$

By neglecting the fluctuations [11], one then arrives at the approximate evolution equation of the average angle

$$\frac{d\bar{\theta}}{dt'} = h^2 \sin[2(\theta_H - \bar{\theta})], \quad (4.4)$$

whose solution, for $\bar{\theta}(t'=0) = 0$, is

$$\bar{\theta}(t') = \theta_H - \tan^{-1}[\exp(-2h^2 t') \tan \theta_H]. \quad (4.5)$$

According to Eq. (4.5), the (unnormalized) relaxation time τ_H is inversely proportional to the square of the applied magnetic field

$$\tau_H = \frac{1}{Dh^2}. \quad (4.6)$$

This H^{-2} power law is in agreement with the experimental findings [5–7]. In Sec. V we shall perform a quantitative comparison of our theoretical predictions with the experimental data obtained by Oliveira and co-workers [5–7].

In Fig. 2 we show the steady-state probability P_s obtained by numerical integration of Eq. (3.2) in the absence of magnetic field, for two values of the normalized elastic constant

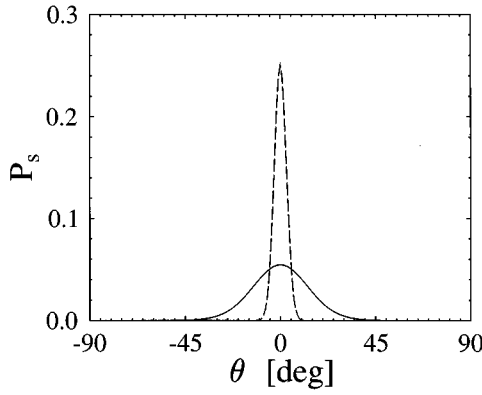


FIG. 2. Steady-state probability distribution P_s for $h=0$, $\delta=\pi/100$, and two different values of κ : ($\kappa=10$, solid line; $\kappa=200$, dashed line). The numerical solution of the master equation and the analytical result of the Fokker-Planck approximation coincide.

($\kappa=10$, solid line; $\kappa=200$, dashed line). The average twist angle $\bar{\theta}$ is evidently arbitrary and depends solely on the initial conditions. For δ sufficiently small (here $\delta=\pi/100$) this numerical solution practically coincides with the analytical solution (4.1) of the Fokker-Planck continuum approximation. According to Eqs. (3.14) and (4.1), the width of the steady-state distribution is inversely proportional to the square root of the elastic constant.

The time evolution of the average twist angle $\bar{\theta}$ is shown in Fig. 3 for different values of the normalized magnetic field h and normalized elastic constant κ and for the same value $\delta=\pi/100$ as before, with $\theta_H=\pi/4$ and $\bar{\theta}(t'=0)=0$, where $t'=Dt$ is the previously defined normalized time. The initial probability distribution $P(t'=0, \theta)$ is taken as the steady-state solution $P_s(\theta)$ in the absence of a magnetic field. In Fig. 3(a) the amplitude of the normalized magnetic field is $h=1$. The long (short) dashed line is the numerical solution corresponding to $\kappa=10$ ($\kappa=200$). The solid line is the analytical approximate solution (4.5) of the Fokker-Planck equation: it does not depend on κ , i.e., on the width of the steady-state distribution, since we neglected the fluctuations in deriving Eq. (4.5). As it is evident, the relaxation time somehow depends on κ . However, this effect can be taken into account by simply rescaling the magnetic field h : this is shown by the circles in Fig. 3(a), which correspond to the analytical solution (4.5) with $h'=0.95h$. This rescaling is h independent, as shown in Fig. 3(b), in which $h=0.1$. The insets in Fig. 3 show the probability distribution for three successive values of time. For larger values of the magnetic field h , the drift of the distribution is accompanied by a squeezing, while for smaller h the evolution is practically a rigid translation. This is evident from Eqs. (3.14) and (4.1), which show that under stationary conditions, where $\bar{\theta}=\theta_H$, the width of the distribution is inversely proportional to $\sqrt{h^2+\kappa}$. However, as we shall see in the following, in practical cases $h^2\ll\kappa$ and therefore the field-induced squeezing of the probability distribution is completely negligible.

V. TEMPERATURE BEHAVIOR AND COMPARISON WITH THE EXPERIMENTAL DATA

The experimental data of the time evolution of the surface director gliding show a rather strong dependence of the re-

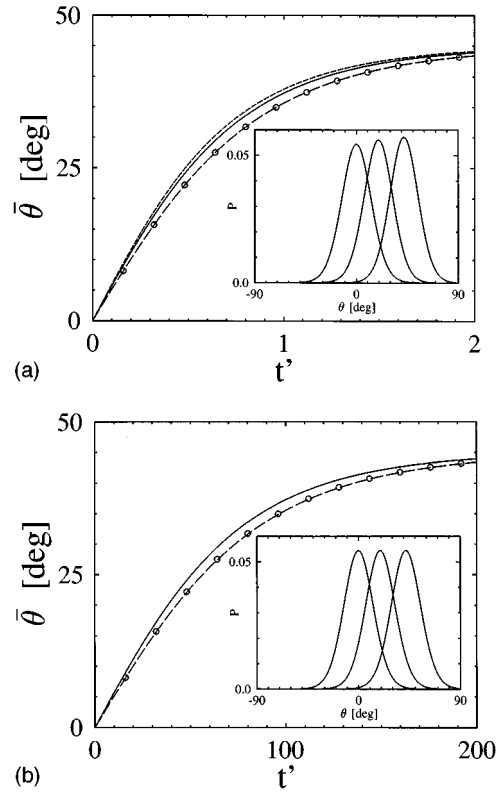


FIG. 3. Time evolution of the average twist angle $\bar{\theta}$ as a function of the normalized time t' for $\delta=\pi/100$ and $\theta_H=\pi/4$. (a) $h=1$ with $\kappa=10$ (long-dashed line) and $\kappa=200$ (short-dashed line). The solid line (circles) is the analytical solution (4.5) with $h'=0.95h$. The inset shows the probability distribution $P(\theta, t')$ corresponding to the long-dashed curve as a function of θ for $t'=0, 0.4$, and 1.6 (from left to right). (b) Same as (a), but for $\kappa=10$ and $h=0.1$ (long-dashed line); the analytical solution is plotted for $h=0.1$ (solid line) and $h=0.095$ (circles). The probability distributions in the inset are for $t'=0, 41$, and 163 (from left to right).

laxation time τ_H on temperature, close to the first-order clearing point T_c (see Table II of Ref. [6]). This dependence cannot be explained by the temperature variation of the diamagnetic anisotropy χ_a : in fact, according to Eq. (4.6), $\Delta\tau_H/\tau_H = -\Delta\chi_a/\chi_a$. Now χ_a decreases as the temperature increases, in a way essentially proportional to the bulk nematic order parameter S [1]; this would therefore give an increase in the relaxation time τ_H with temperature, contrary to what is observed experimentally [6]. Moreover, for typical variations of the nematic order parameter [1], the effect due to the temperature variations of χ_a is about 20 times smaller than the observed temperature variations of τ_H .

In order to explain this temperature dependence, we assume that the depth of the potential well u_0 [see Eq. (3.5)] depends on the nematic order parameter S . In the isotropic phase $S=0$, we expect $u_0=0$. For increasing values of S we expect u_0 to increase. Therefore, by expanding u_0 in power series of S , the leading term expansion will be simply

$$u_0 = \alpha S. \quad (5.1)$$

This mean-field approximation is similar to the behavior for the angular anchoring energy proposed in Ref. [12].

In the nematic phase, for $T < T_c$, S is approximatively given by [13]

$$S = \Delta \sqrt{1 - \frac{T}{T_0}}, \quad (5.2)$$

where $T_0 - T_c \cong 1^\circ\text{C}$ [1]. From Eqs. (5.1) and (3.7), neglecting the small temperature dependence of χ_a , at first order in $T - T_c$ the characteristic diffusion time τ varies with temperature according to the linear dependence

$$\tau(T) = \tau(T_c) + \beta(T - T_c), \quad (5.3)$$

where

$$\beta = \frac{\tau(T_c)}{2(T_0 - T_c)} \ln \left[\frac{\tau_0}{\tau(T_c)} \right]. \quad (5.4)$$

Consequently, the temperature dependence of the magnetic relaxation time (4.6) describing the surface director gliding is written

$$\tau_H(T) = \tau_H(T_c) + \beta_H(T - T_c), \quad (5.5)$$

where

$$\beta_H = \frac{\beta}{\delta^2 h^2}. \quad (5.6)$$

The experimental results reported in [6] give $\beta_H \cong -56 \text{ s}/^\circ\text{C}^{-1}$ for $H = 8 \text{ kG}$. According to [14], $\chi_a = 10^{-8}$ (cgs units), while the molecular density $n = 1/Al$ is of the order of $n \cong 3 \times 10^{19} \text{ cm}^{-3}$ [15]. Therefore, for $H = 8 \text{ kG}$ we have $h^2 \cong 2.6 \times 10^{-7}$. We note also that $l \cong 60 \text{ \AA}$ [16]; hence, with the elastic constant $K \cong 10^{-6} \text{ dyn}$, $\kappa \cong 8$. We can estimate the elementary angular jump δ as the ratio between the distance p between two pinning centers and the length L of a micelle; taking $p \cong 2 \text{ \AA}$ and $L \cong 100 \text{ \AA}$ [16], one obtains $\delta \cong p/L \cong 2 \times 10^{-2} \text{ rad}$. The trial frequency τ_0^{-1} is of the order of the molecular vibration frequencies, $\tau_0^{-1} \cong 10^{14} \text{ Hz}$ [17]. With these values, from Eq. (5.6) we get $\beta \cong -5.8 \times 10^{-9} \text{ s}/^\circ\text{C}^{-1}$; consequently, from Eq. (5.4), we have $\tau(T_c) \cong 10^{-9} \text{ s}$. Hence, at $H = 8 \text{ kG}$, $\tau_H(T_c) = \tau(T_c)/\delta^2 h^2 \cong 9.7 \text{ s}$. For $T_c - T = 4^\circ\text{C}$, then $\tau_H(T) \cong 234 \text{ s}$, in good agreement with the experimental value $\tau_H(T) \cong 250 \text{ s}$ reported in Ref. [6]. The comparison with the full data presented in Ref. [6] is shown in Fig. 4. We note also that with these data at $T = T_c$ we get a depth of the potential well per micelle of the order of $u_0 K_B T \cong 0.3 \text{ eV}$, which is a reasonable value for the interaction energy between one micelle and the substrate.

VI. CONCLUSION

In this paper we have proposed a microscopic description of the surface gliding effect recently observed in lyotropic liquid crystals in contact with amorphous solid substrates. This model is based on the theory of thermally activated processes. The micelles are supposed to be pinned at the

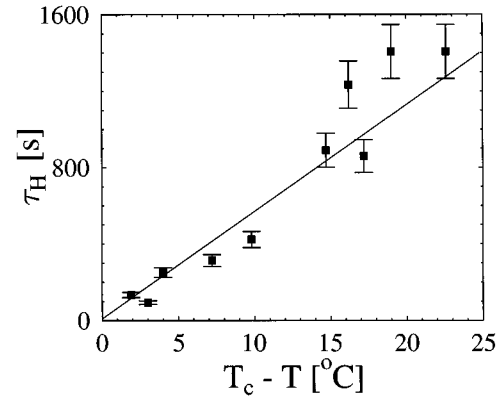


FIG. 4. Comparison between the experimental data (squares) and the theoretical prediction (full line) for the relaxation time τ_H as a function of temperature. The error bars represent a 10% error on the experimental data.

surface by a periodic potential having equally spaced minima separated by barriers having the same height. The application of an external magnetic field induces a critical state that does not correspond to an equilibrium situation and therefore tends to relax. This phenomenon is well known in the case of magnetism as an ‘‘aftereffect’’ or ‘‘magnetic viscosity’’ and in the case of superconductivity as the ‘‘creep of flow’’ [18].

We have given a formulation of the gliding process in terms of a master-equation describing the jumps between adjacent angular positions. In the continuum limit the master equation reduces to a Fokker-Planck partial differential equation. Its steady-state solution gives the expected Boltzmann distribution, whereas the time evolution for the average orientation has been obtained approximately by suitably neglecting the fluctuations. A comparison between the numerical solution of the master equation with the approximate analytical results has shown the substantial correctness of the latter. The relaxation time has been found to be inversely proportional to the square of the applied magnetic field, as experimentally observed. We have also developed a simple mean-field description of the surface pinning potential that is able to reproduce the observed temperature dependence of the relaxation times.

A possible extension of our model is to consider a distribution of barrier heights centered around some mean value: such a distribution is expected to modify the details of the time evolution of the average orientation, but not to change considerably the dependence of the relaxation time on the applied magnetic field. Our model could also be extended to Berreman-like geometric anchorings [19], where the surface anchoring has a geometrical contribution connected to the topography of the surface. In this case the pinning potential should be substituted by the total elastic energy connected with different surface geometries.

ACKNOWLEDGMENTS

A.K.Z. acknowledges partial support from Politecnico di Torino in the framework of the scientific collaboration between Politecnico di Torino and Russian Academy of Sciences. We thank C. Oldano, A. M. Figueiredo Neto, and G. Durand for useful discussions.

- [1] J. Prost and P. G. de Gennes, *The Physics of Liquid Crystals* (Clarendon, Oxford, 1993).
- [2] J. Charvolin, *Nuovo Cimento D* **3**, 3 (1984).
- [3] See, e.g., B. Jérôme, *Rep. Prog. Phys.* **54**, 391 (1991).
- [4] S. Faetti and M. Nobili, *Phys. Lett. A* **217**, 133 (1996).
- [5] E. A. Oliveira, A. M. Figueiredo Neto, and G. Durand, *Phys. Rev. E* **44**, R825 (1991).
- [6] E. A. Oliveira and A. M. Figueiredo Neto, *Phys. Rev. E* **49**, 629 (1994).
- [7] R. de F. Turchiello and E. A. Oliveira, *Phys. Rev. E* **54**, 1618 (1996).
- [8] A. Tanguy and Ph. Nozières, *J. Phys. (France) I* **6**, 1251 (1996).
- [9] See, e.g., E. S. R. Gopal, *Statistical Mechanics and Properties of Matter: Theory and Applications* (Horwood, Chichester, 1974).
- [10] F. C. Frank, *Discuss. Faraday Soc.* **25**, 19 (1958).
- [11] See, e.g., C. W. Gardiner, *Handbook of Stochastic Methods: For Physics, Chemistry and the Natural Sciences* (Springer, Berlin, 1983).
- [12] Ping Sheng, *Phys. Rev. A* **26**, 1610 (1982).
- [13] E. B. Priestley, P. J. Wojtowicz, and Ping Sheng, *Introduction to Liquid Crystals* (Plenum, New York, 1974).
- [14] T. Kroin and A. M. Figueiredo Neto, *Phys. Rev. A* **36**, 2987 (1987).
- [15] E. Zhou, M. Stepanov, and A. Saupe, *J. Chem. Phys.* **88**, 5137 (1988).
- [16] Y. Galerne, A. M. Figueiredo Neto, and L. Liebert, *J. Chem. Phys.* **87**, 1851 (1987).
- [17] G. Herzberg, *Spectra of Diatomic Molecules* (Van Nostrand, Princeton, 1950).
- [18] P. G. de Gennes, *Superconductivity of Metals and Alloys* (Benjamin, New York, 1976).
- [19] D. W. Berreman, *Phys. Rev. Lett.* **28**, 1683 (1972).